



OPEN

Gradient Control of the Adhesive Force between Ti/TiO₂ Nanotubular Arrays Fabricated by Anodization

SUBJECT AREAS:
STRUCTURAL PROPERTIES
MECHANICAL PROPERTIES

Minghui Zhao, Jidong Li, Yubao Li, Jian Wang, Yi Zuo, Jiaxing Jiang & Huanan Wang

Received
19 August 2014Accepted
5 November 2014Published
24 November 2014Correspondence and
requests for materials
should be addressed to
J.L. (nic1979@scu.
edu.cn)

Research Center for Nano-Biomaterials, Analytical & Testing Center and State Key Laboratory of Biotherapy West China Medical School, Sichuan University, Chengdu, 610064, China.

The poor control of the adhesion of TiO₂ nanotubes (TNTs) layers to a non-anodized titanium (Ti) substrate has limited their widespread application, because the stripping mechanism has not yet been revealed. Here, we report a novel method to control the detachment of TNTs by post-treatment of the as-fabricated samples in protic and aprotic solvents with different polarities. Post-treatment using an organic solvent of lower polarity increases the adhesion of the tube layer, in contrast to the spontaneous detachment of the TNT layer after treatment using a solvent of higher polarity. The structure and the composition at the rupture interface were studied to explore the mechanism of the stripping behavior. Based on our experimental results and previous studies, a hypothesis of a hydrogen-assisted cracking (HAC) mechanism was proposed to explain the mechanism of TNTs' natural detachment and the control over of TNTs' stripping behaviors by post-treatment, in which the presence of protons at the interface between the TNT layer and the Ti substrate play an important role in controlling the two layers' cohesion. In summary, this method and mechanism hold promise to be used as a tool for the design and fabrication of TNT-related materials in future.

TiO₂ nanotubes (TNTs) prepared by an anodizing process have recently attracted intensive interest due to their promising applications in the fields of photocatalysis¹, hydrogen storage², water purification³, biomedical materials⁴, tailored wettability⁵, etc. To improve properties, TNTs with various morphologies, such as double-layered and bamboo-shaped TNTs⁶, were fabricated by tailoring the preparation parameters. Mor et al.⁷ fabricated an independent TNT array without a substrate by sputtering ultrathin Ti onto fluorine-doped tin oxide coated glass anode, which provided more opportunities to research TNTs in solar cells. In contrast, with regard to many other applications such as surface treatment of titanium implants for biomedical use, stable TNT layers with strong cohesion to Ti substrates were preferred owing to the desirable biocompatibility and the capacity for drug delivery of the TNT layer⁸. However, the tubular structure could be spontaneously stripped off just after the end of the anodization when the intratubular electrolyte volatilized, which absolutely hampered its widespread application.

In that aspect, the mechanism controlling the TNTs' stripping is important. Zhou et al.⁹ have described excellent research on the formation and the microstructures of TNTs, and proposed that the separated nanotubes could be formed by the volume shrinkage of the hydroxide layer at the tubes' bottom. Additionally, Schmuki et al.¹⁰ proposed that the adhesion of TNTs to the Ti substrate was controlled by the fluoride-rich layer, which could be improved by carbonization¹¹. Schmuki et al. also emphasized that the mechanical stability of the tube layers should be clearly addressed but has not yet been extensively studied¹⁰. Furthermore, to satisfy any intended application, we should find some parameter that can adjust the adhesive force between the porous oxide layer and the substrate. Luckily, Lin's group¹² has reported a simple and safe way to peel off the TNTs' layer by washing in methanol. It was shown that the freestanding and close-packed nanotubes can provide good performance in dye-sensitized solar cells (DSSCs). However, approaches to anchor the tube layers are still not clear from the available literature. In addition, there is still the lack of a detailed mechanism to explain the methanol-induced delamination of the TNTs' barrier layer. Herein, based on the prior experimental results, we designed a series of experiments to confirm the effect of washing solvents on the TNTs' adhesive force with the substrate, which enabled control over the stripping process.

TNTs were fabricated in the classical ethylene glycol (EG)/NH₄F systems with voltage of 60 V applied. As shown in Fig. 1, the diameter of the nanotubes fabricated in this study is approximately 120 ~ 130 nm with a considerably high-aspect-ratio of approximately 200 : 1. These freshly anodized TNTs turned out to be unstable

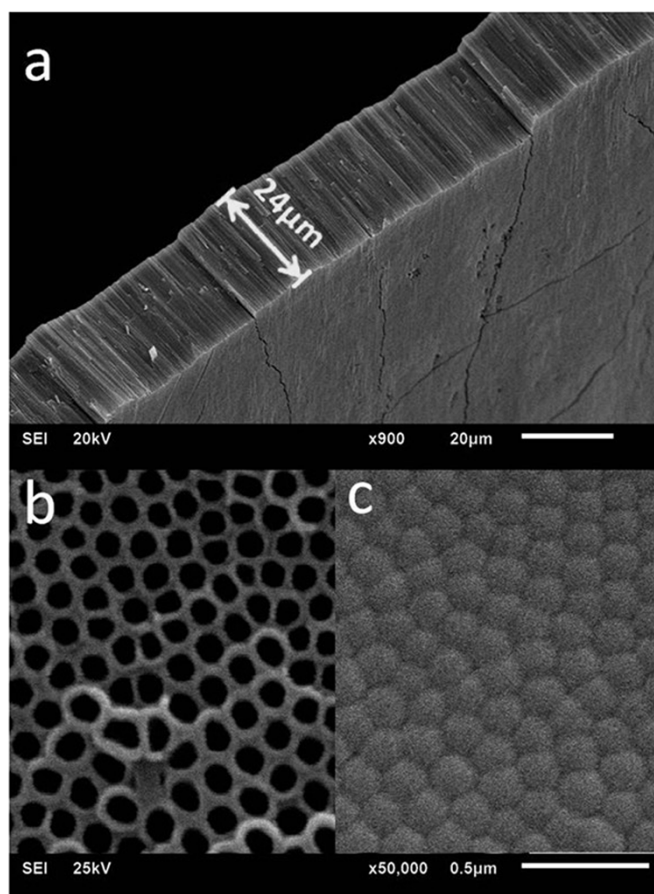


Figure 1 | Lateral (a), top (b) and bottom (c) view SEM images of TNTs peeled from the titanium substrate.

in adhering to Ti substrates. However, we found that being immersed in aprotic solvents with lower polarity, such as petroleum ether, could increase the TNTs' adhesive force, while the strongly polar protic solvents such as methanol could apparently induce the detachment. The interfaces where the fracture occurred were studied by transmission electron microscopy (TEM), atomic force microscopy (AFM) and X-ray photoelectron spectroscopy (XPS). Apart from the acidic micro-environment in the nanotubes reported in the literature^{13,14}, titanium hydrides were found in the bottom layer of the TNTs in our study. Therefore, the hydrogen-assisted crack (HAC) mechanism was reasonably used to demonstrate the stripping behavior of the TNT layers from the Ti substrate. We found Ti-H and hydrogen blisters may directly influence the interfacial cohesion between the tubular layers and substrates, especially the inner hydrogen blistering process which could engender high pressure, increasing the tendency of the separation of the tube layer. All of these will be shown in the following and be used to explain the mechanism of TNTs' stripping process persuasively.

Experimental Section

Self-assembled TiO₂ nanotube arrays were fabricated by anodization at a voltage of 60 V supplied by a direct current (DC) power supply, employing a classical ethylene glycol/NH₄F system containing 3 vol% H₂O, 0.5 vol% H₃PO₄ and 0.3 wt% NH₄F as electrolyte. The anodization time was set at 5 hours. Eight pure organic solvents with different polarities were used for the post-treatment of the freshly fabricated TiO₂ nanotube arrays. The samples were immersed for 15 min, after which the adhesive force between the TiO₂ nanotubes (TNTs) layer and the Ti substrate was characterized by Revetest Scratch Tests. SEM, AFM and XPS depth profile analysis were used to characterize the micro-structure and compositions of the distinct interfaces of naturally and mechanically stripping TNT samples.

Revetest Scratch Tests. The as-fabricated TNTs specimens were dried at room temperature. The samples were fixed on the Revetest Scratch Tester (HH-3000) and

then the force was loaded from 0 to 100N. During the detection, the tester's needle scratched through a 5-mm-long region, having the loading force increased from 0 to 100 N, at a rate of 20 N/mm. When the tip of the needle cut the brittle thin film on the substrate, an acoustical signal was received and peaks would appear simultaneously on the graphs. Taking the first acoustical signal peak as the standard, the adhesive strength between TNTs and substrate could be represented.

XPS Depth Profile Analysis. The superficial nanotubes' layer of the anodized samples was removed and the remaining substrate was washed in deionized water. The specimens were scanned and the spectrum data were collected after every etch (by Ar⁺ sputtering for 2 min), repeated seven times in all. The test was used to analyze the delicate variation of the composites among the barrier layer.

Results and Discussion

Titanium plates with a size of 15 mm by 20 mm by 4 mm, Grade 2 purity, were anodized under particular conditions and assembled clean TNT arrays successfully. However, the common EG/NH₄F electrolyte may cause the formation of a cracked and irregular "nanograin" surface¹⁵, while TNTs with a smooth top view have been successfully fabricated^{16,17}. Additionally, Schmuki et al.¹⁸ reported that the content of H₂O might influence the appearance of "nanograin". Here we used a modified formulation with H₃PO₄ added to clean the top surface of the TNTs. Increasing the acidity of the electrolyte might etch the covering on the top of the tubes and thus induce a better appearance.

In the present study, the freshly fabricated TNTs were immersed in different organic solvents for a post-treatment. Here, we used the TNTs immediately immersed in deionized water, without any other post-treatment, as the control group, because the composition of electrolyte in the tubes was too complicated to attain stable adhesion. After the post-treatment, there existed a distinct differentiation of the TNTs' adhesive force to the Ti plates. Among the organic solvents, the specimens treated by methyl alcohol stripped spontaneously without any applied force, which was consistent with Lin's results¹². What is more, as shown in Fig. 2a (also see Supplementary Figure S1, S2 and Supplementary Table S1), the results of the Revetest Scratch tests proved that the gradient control of the TNTs' adhesive strength with the Ti substrates has been achieved simply by the post-treatment of the as-fabricated TNT samples with different solvents. The eight organic solvents have a distinguishable effect on the adhesive strength, even completely opposite, e.g., 'petroleum ether' and 'methyl alcohol'. It was also found that aprotic solvents were much better than protic solvents in the ability to fix the barrier layer. For example, petroleum ether, an aprotic solvent, demonstrated a significant effect in strengthening adhesion. Only when the force was loaded to approximately 58 N, could the oxide layer separate from the Ti plate. On the contrary, TNT layers treated with protic solvents, e.g., n-butyl alcohol, isopropyl alcohol and methyl alcohol, show lower adhesive force. The same specimen post-treated by a protic solvent (methyl alcohol) and an aprotic solvent (acetone) exhibited considerably different stripping behaviors of the TNT layer (see Supplementary Figure S3), which was difficult to explain by Lin's assumption¹² of solvent-evaporation-induced delamination, because acetone would be much more volatile than methyl alcohol. We found that the TNTs' adhesive strength to the substrate as an effect of soaking in solvents was related to the polarity of those solvents, i.e., the lower polarity of the organic solvent used to treat the as-fabricated TNT samples, the higher the adhesive force between the TNT layer and the Ti substrate achieved. Moreover, aprotic solvents were generally better than protic ones in strengthening the adhesive force of the oxide layers. In addition, it was also found that the control group (treated in H₂O) exhibited similar results to those immersed in protic organic solvents because the H₂O is also a protic solvent. A possible explanation for this phenomenon could be that the protic solvents were influenced by the H⁺ remaining in tubes, which increased the dipole moments and turned them into strongly polar solvents.

Based on the abovementioned results, it was concluded that some solvents with low polarity such as petroleum ether and cyclohexane

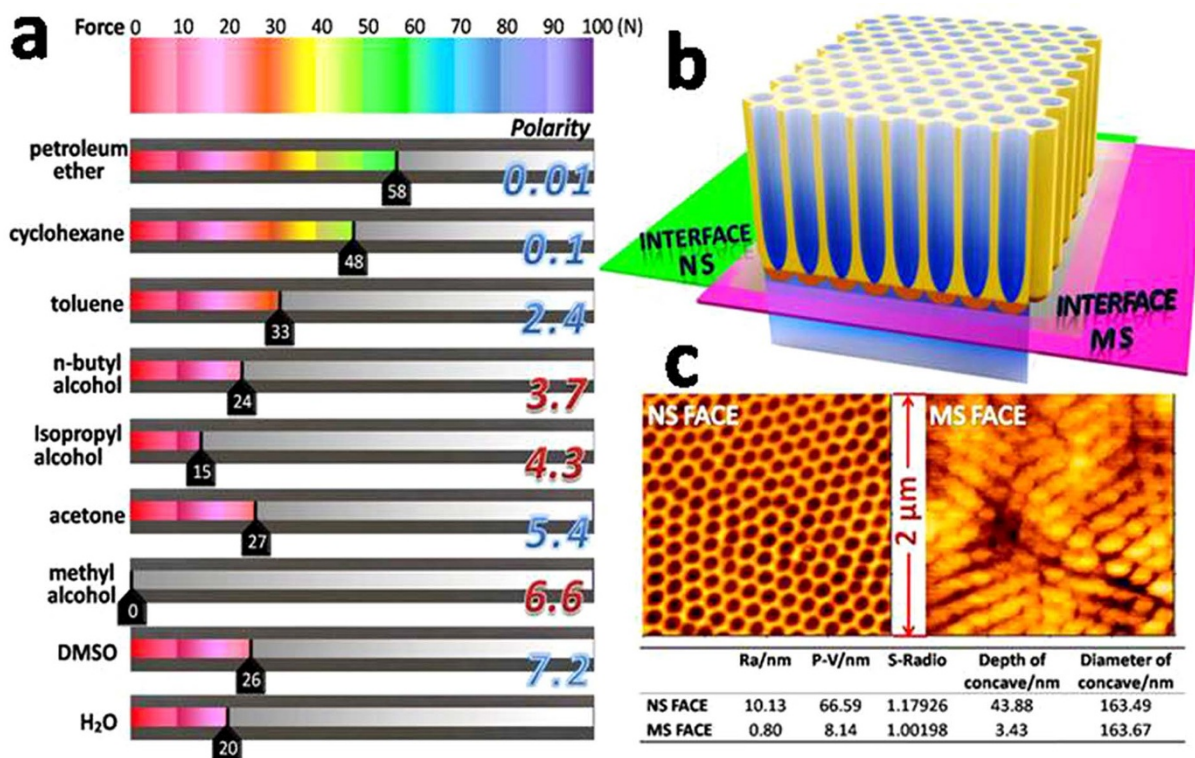


Figure 2 | (a) The average value of the loading force applied in three parallel Revetest Scratch tests performed for each sample. Eight organic solvents, aprotic or protic (polarity from 0.01 to 7.2), were adopted to post-treat the freshly fabricated TNTs, with samples washed by H₂O as a control. (b) Schematic diagram for interfaces naturally stripping and mechanically stripping. (c) AFM photos of NS face and MS face.

could strengthen TNTs' adhesion with the substrate. It is notable that for use in different applications, the crystal structure phase of the TNTs, such as the anatase phase, is important and annealing as a post-treatment will be necessary. What is more, the annealed TNTs not only showed good properties in photocatalysis^{19,20} but also exhibited increased hardness and Young's modulus^{21,22}. Here, we employed a tensile test to check whether the strengthening effect caused by the organic solvents would be kept. The results and details of the experimental method are shown in Supplementary Fig. S4. We found the specimens treated by cyclohexane (polarity of 0.1, aprotic solvent) show a higher adhesive strength than those treated by isopropyl alcohol (polarity of 4.3, protic solvent) at room temperature. Nevertheless, after 500 °C annealing of the post-treated samples, both groups of TNTs transformed into anatase crystals and shared a similar but higher adhesive force with the substrate. The annealing treatment really enhanced the adhesive force¹¹, and the limiting point of this force turned out to be the anatase TNTs itself rather than the barrier layer. The X-ray diffraction (XRD) result showed that TNTs treated at 500 °C presented a good anatase phase, while the tensile test evidenced the post-treatment could satisfy the demand for adhesion and integrity, which means this facile method would also be helpful for improving the quality of the anatase or rutile TNT films. However, more comprehensive research into the mechanics of TNTs after different annealing conditions is still in process.

To further study the influence of the solvents' polarity on TNTs' adhesion, two extreme conditions were investigated, in which a TNTs sample treated with cyclohexane with a low polarity of 0.1 was compared to a sample treated with methyl alcohol with a higher polarity of 6.6. For the sample treated by methyl alcohol, the TNT layer naturally peeled off (hereby named as naturally stripping (NS)), in contrast to the formation of a TNT layer firmly adhered to the substrate treated with cyclohexane. The TNT layers of the latter sample were peeled off passively (hereby named as mechanically stripping (MS)) (Figure 2b) using tape (with initial adhesion more

than 10 N/inch) for further study. Moreover, the surfaces of the remaining substrates with tube layers peeled off were further observed with AFM (Figure 2c), which displayed the obviously difference in morphology of the substrate surfaces resulting from the naturally stripping (NS FACE) and the mechanically stripping (MS FACE) processes. The NS FACE showed a morphology featuring tube structures with an average depth of the "pores" of 43.88 nm, which was similar in appearance to the image shown in Fig. 1b, but actually consisted of shallow caves rather than tubes (see Supplementary Figure S5). In contrast, the MS FACE only has average depth of 3.43 nm for every cell. Additionally, the two faces showed similar cell diameters of 165 ± 10 nm, in line with that of the nanotubes. Furthermore, the SEM images of the bottom of the stripped TNT layers confirmed the corresponding trends (see Supplementary Figure S6). In general, we can assume that the two fracture interfaces (MS and NS) possessed different mechanical strength. When compared to the stretching resistance at the MS interface, the adhesive strength at the NS interface turned out to be flexible and controllable, that is, the impact of the soaking solvents was totally exerted on the NS interface.

To investigate the mechanism of the TNTs' detachment behavior, XPS deep inspection was originally employed to examine the variations of the physicochemical properties of the NS and MS interfaces as a function of surface depth. What is more, this XPS deep inspection was utilized as a creative and powerful approach to detect the chemical bonding and complicated compositions of the barrier layer, which was complementary with the previous TEM characterization²³. As shown in Fig. 3, obvious differences can be observed in the variations of the chemical bonds between the NS and MS interfaces with the increase of etching depth. This is understandable because the barrier layer of TNTs is usually regarded as a transition area from titania to titanium due to the electrochemical corrosion of barrier layer during the anodization process for TNT fabrication²⁴. In the present study, the differences in the XPS profiles can be



accounted for by two aspects: (i) the different fracture interface resulting from the MS or NS process (See Figure 2b and Supplementary Figure S6) and (ii) the compositions of the inner and outer parts of the barrier layer. Zhou et al.²³ have recently reported that the barrier layer can be divided into amorphous oxide (TiO_2 , inner part) and hydroxide ($\text{TiO}_2 \cdot x\text{H}_2\text{O}$, outer part) layers by TEM examination. And Schmuki et al.²⁵ have indentified the existence of $\text{Ti}(\text{OH})_4$ by XPS in the barrier layer. Our results here concurred with Zhou's double-layer microstructure (see Supplementary Figure S7) and Schmuki's finding of Ti-OH, but further explored the phase of TiH_2 exactly.

For the MS interface (Figure 3a and 3b), with the increase of etching time from 1 to 7, the peaks of Ti 2p were wide, especially at a depth of 10 ~ 50 nm (Figure 3b). These peaks ranged from 453 to 465 eV and corresponded to the phases of Ti ($\text{Ti } 2p_{3/2}=454.1$ eV, $\text{Ti } 2p_{1/2}=460.1$ eV), TiH_2 ($\text{Ti } 2p_{3/2}=453.3$ eV, $\text{Ti } 2p_{1/2}=459.1$ eV)²⁶, and TiO_x (see Supplementary Figure S8). Among these peaks, the peaks at 453.3 and 459.1 eV gradually became prominent with an increase of the etching depth, which means a component of TiH_2 appeared to be concentrated near the NS interface. Combined with Fig. 3b, the major form of O resulted from TiO_x , and the value of x reduced with the increase of etching depth (see Supplementary Figure S8). However, one point should be addressed that the minor peaks at 531.9 eV, 532.0 eV, which corresponded to bridge-bond-O (BBO) and bridging -OH (BOH), respectively^{27,28}, did not vanish with an increase of the etching depth. Moreover, the spectrum of O 1s indicated the existence of abundant oxygen vacancies within the barrier layer due to the severe partial oxidation. Additionally, a recent report²⁹ demonstrated that molecular hydrogen could be produced by BOH with plenty of existing oxygen vacancies. Thus we can speculate that conditions contributing to a tiny amount of H_2 generation at the barrier layer of TNTs between the MS interface and NS interface existed.

For the NS interface (Figure 3c and 3d), the profiles after the first 4 minutes of etching indicated that Ti was the major phase, as evidenced by the normalized Ti^0 peak ($\text{Ti } 2p_{3/2}=454.1$ eV, $\text{Ti } 2p_{1/2}=460.1$ eV)³⁰ with a tiny amount of O belonging to lattice oxygen atoms and organic solvents ($\text{O } 1s=531.3$ eV-531.6 eV, 533.7 eV). This is due to the treatment with methyl alcohol, which resulted in spontaneous disintegration of the anodized TiO_2 layer from the Ti substrate, leaving the NS surface mainly composed of Ti. Surprisingly, the O 1s peak at 533.7 eV corresponds to $-\text{CH}_2-\text{OH}$ ³¹, caused by the composition of the electrolyte (EG) used for the anodization of TNTs. This strongly demonstrated the existence of permeable nanoscale channels across the barrier layer for the penetration of electrolyte molecules or some other small molecule substances. In summary, these results suggested that the remaining material can be considered as pure titanium after NS.

Comparing the XPS compositional analysis of the MS and NS interfaces, we found similarities in the phases of Ti ($\text{Ti } 2p_{3/2}=454.1$ eV, $\text{Ti } 2p_{1/2}=460.1$ eV), TiO_x (see Supplementary Figure S8), BBO, and BOH ($\text{O } 1s$, 531.9 eV). However, differences between the two contrasting samples could be summarized as: (i) the major peaks of Ti 2p and (ii) bonding of titanium and oxygen atoms. The spectrum of Ti 2p in 'MS' shifted to a lower binding energy due to the formation of TiH_2 . TiO_x of the MS specimen still could be regarded as the products of the beginning oxidation, but the deep components in the NS specimen turned out to be a single, consistent species (also see Supplementary Figure S8c and S8d), which should be the native dissolved oxygen atoms in metallic Ti.

To our knowledge, titanium has strong capacity for the dissolution of hydrogen, and the interstitially dissolved hydrogen can transform into titanium hydrides (Ti-H) with an increase of the hydrogen concentration³³. This process consequently reduces the toughness of Ti³⁴. Therefore, the titanium hydrides in the barrier layer would be efficient in enhancing the brittleness of the materials and accel-

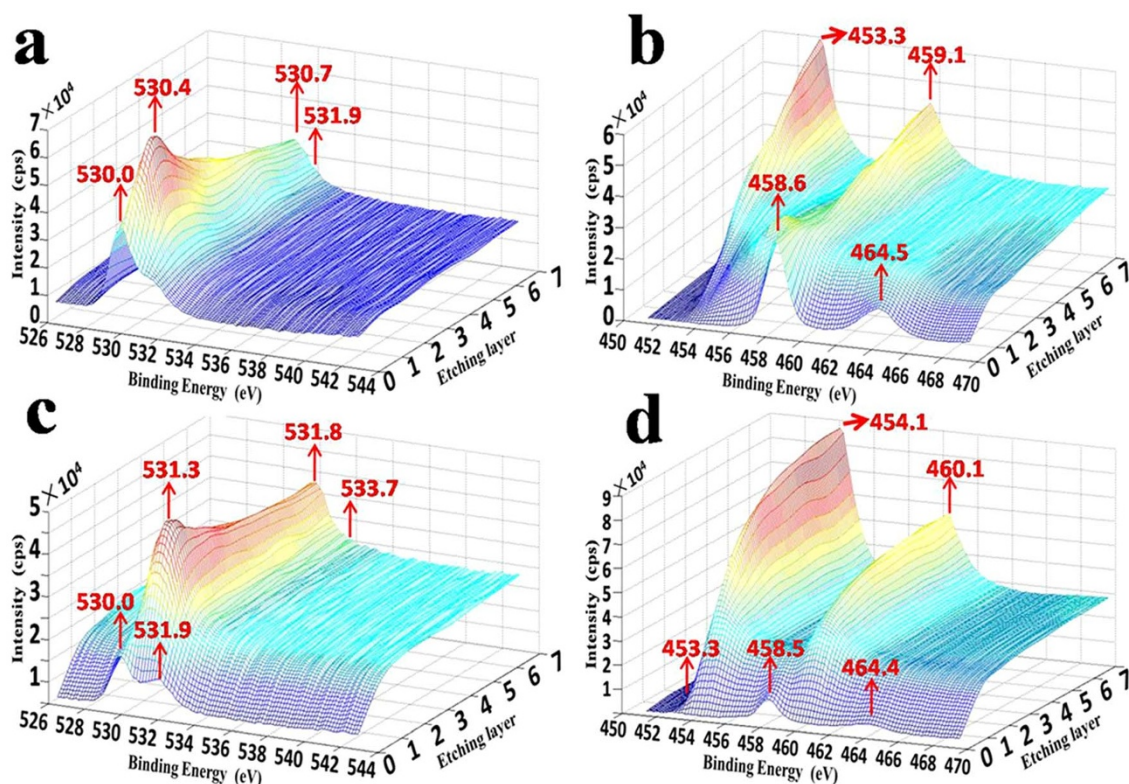


Figure 3 | XPS depth profile of remaining substrate after naturally and mechanically stripping: XPS spectrum of (a) O in MS, (b) Ti in MS, (c) O in NS, (d) Ti in NS. Ar^+ sputtering etched every specimens seven times for 2 min at a time (sputtering etch rate approximately 5 nm/min³²).

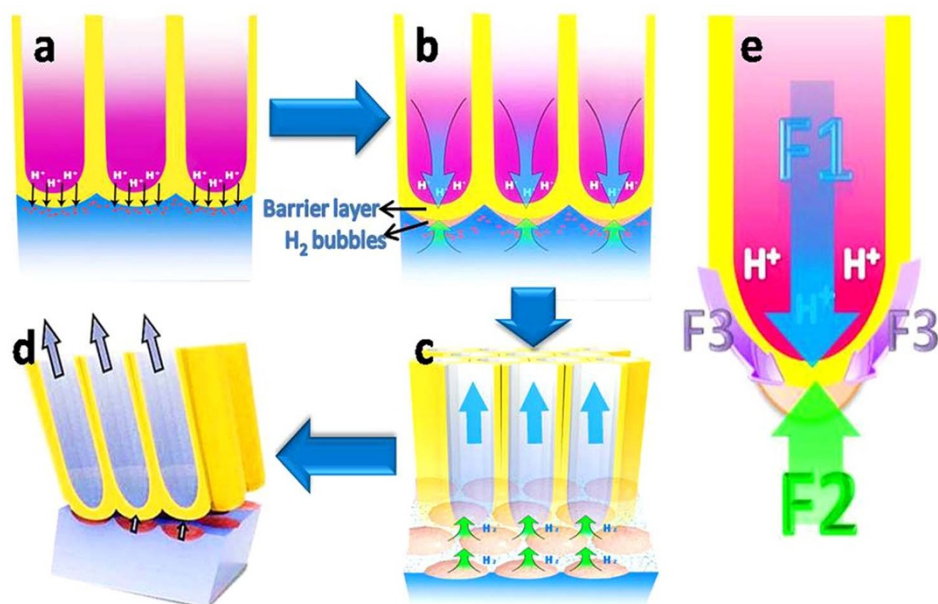
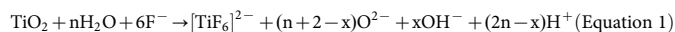


Figure 4 | Schematic diagrams for TNTs' naturally stripping mechanism. (a) H^+ pass through the barrier layer, (b) the expansibility of H_2 bubbles and the fluid pressure from the solution in tubes are in opposition to each other, (c) mechanical equilibrium is broken after electrolyte volatilization and nanoscale cracks appear at the barrier layer/Ti substrate interface and increase rapidly, (d) the TNT layer peels off, (e) force analysis of the barrier layer.

erating the potential rupture. This speculation is consistent with previous literature³⁵ about hydrogen embrittlement and our experimental data.

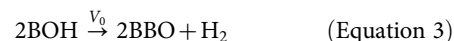
It was reported that H^+ was generated in the nanoporous structure during the anodizing process, and the reaction can be written as equation 1³⁶:



The large amount of H^+ normally gathers at the bottom of the resultant tubes, forming a pH gradient in TNTs¹⁴ and further increasing the depth of the tubular structure resulting from the H^+ corrosion. Therefore, the generated H^+ diffusion to the external environment from the bottom of the TNTs would be impeded by high viscosity electrolytes, which can make the internal tube environment fall into a semi-isolated state. Freshly fabricated TNTs can release inner H^+ into the outer environment very slowly, supporting this assumption (see Supplementary Figure S9), which is consistent with previous reports^{13,14}. The abundance of H^+ at the bottom of TNTs could pass through the barrier layer under the fluid and osmotic pressure applied by the electrolyte, and then infiltrate into the superficial titanium substrate (as described in Figure 4a). The contact between the TiO_2 nanotubes layer (n-type semiconductor³⁷) and the metallic Ti can form a built-in electric field pointing to the Ti substrate (the built-in electric field could exist in the junction of n-type semiconductor and the metal³⁸). This field-aided diffusion could become another reason for the permeation of H^+ . And then the titanium hydrides shown in XPS analysis profiles (see Figure 3 and Supplementary Figure S8a, S8b) could be formed.

On the other hand, massive oxygen vacancies exist (see Figure 3a, 3b and Supplementary Figure S8) in the so-called Schottky barrier formed by the barrier layer of the TNTs and the metal substrate³⁹. Therefore, the hydrogen which permeated across the barrier layer may react in three ways: (i) bonding with the Bridge-bond-O (BBO) to form bridging $-OH$ (BOH)²⁹ (see equation (2)); (ii) forming titanium hydrides, e.g., TiH_2 ; (iii) combining with oxygen vacancies to form oxygen complexes which, in turn, could reduce the vacancy-formation energy and thus increase the concentration of oxygen vacancies⁴⁰. The products of these possible reactions (such as BOH and oxygen vacancies) could further serve for the generation of

hydrogen gas (H_2) (see equation (3)). This assumption has recently been supported by Yang et al.²⁹, who found that the continuously rising temperature and existence of a certain concentration of O vacancies (V_o) could facilitate the formation of H_2 molecules at the BOH sites. This necessary condition for H_2 generation coincides with the condition of anodal oxide/titanium interface during the anodizing process caused by electrical energy conversion^{41,42}.



Generally accepted, only the donation of hydrides is difficult to achieve the natural brittle fracture in HAC process without applying external forces. What's more, as shown above, considering hydrogen molecules could be formed at the cracked inclusion or matrix interface, we can assume that hydrogen blisters³⁵ resulting from high-pressure could lead to subcritical cracking³³.

Based on the above principle, during the anodizing process, H_2 molecules could be released continuously by the electrical erosion of the TNTs' barrier or be absorbed by Ti and TiO_2 to form TiH_x and H_2-TiO_2 . Once the anodization process ended, the hydrogen could not be released but entrapped under the barrier layer, which enabled rapid nucleation and the growth of bubbles at the interface between the tube layers and substrate (as described in Figure 4b and Supplementary Figure S10). In this way, a balance can be formed at the barrier layer with upward forces resulting from the expansion of H_2 bubbles (labeled as F2 in Figure 4e), and a downward force due to the hydraulic pressure of the electrolyte solution (labeled as F1 in Figure 4e), and a downward force resulting from the interfacial adhesive force (labeled as F3 in Figure 4e), which assist the system in remaining in a balanced state. Nevertheless, with the volatilization of the electrolyte after the anodization reaction, this balance could be broken due to the gradual decrease of hydraulic pressure and increase of expansion pressure from gas bubbles with the gathering of H_2 , thus leading to the instability of the TNT layer that could be easily detached (Figure 4c, d). Meanwhile, the interfacial adhesive forces that tended to prevent the stripping of the tubular layer could also be



weakened by Ti-H and metalloid impurity segregation^{43,44}. Therefore, the process of TNT layers peeling off automatically can be ascribed to a saltation arising from unbalanced forces.

It was our assumption that by adjusting F1, F2 and F3, the stripping behavior of the TNT layer from the substrate could be controlled. To improve this, we innovatively introduced solvents with a high solubility of H₂ to treat freshly fabricated TNT specimens, to reduce F2 by eliminating H₂ bubbles at the interface between the TNT layer and the substrate, thereby declining the tendency of TNTs' stripping. The immersion of the freshly fabricated TNT specimens into an organic solvent retained the hydraulic pressure (F1) resulting from the solvent, which could keep stable the TNT layer but also facilitate the release of H₂ in form of small molecules into the solvent and buy time for H₂ absorption by Ti and TiO₂, thus reducing F2 and retaining the cohesion of the TNT layer. Therefore, in the current study, solvents with various polarities were tested; it was previously found that the solubility of H₂ has a negative correlation with the polarity of the solvent⁴⁵.

The experimental data perfectly agree with our hypothesis, namely, that solvents of higher H₂ solubility (lower polarity) resulted in a stronger cohesive force of the tube layer and vice versa. The possible existence of permeable channels at the nanoscale across the barrier layer (confirmed by XPS) was also likely to be taken advantage of for the "dissolved-release" of H₂ gas molecules by the organic solvent. Additionally, protic solvents were influenced by the acidic micro-environment, which made them strongly polar solvents and that had difficulty solvating H₂. And thus it was found that an aprotic solvent was much better than a protic solvent to fix the barrier layer.

Conclusions

In summary, the current study proposed a novel and simple method to successfully control the adhesive strength between the TNT layer and the Ti substrate. The stripping behavior of the TNT layer was found to be controllable by a post-treatment using organic solvents with various polarities. It was found that a post-treatment using an organic solvent of lower polarity could increase the adhesion of the tube layer, in contrast to a spontaneous detachment of the TNT layer after treatment using solvent of higher polarity. Moreover, this innovative method and mechanistic study not only enlarged the TNTs' application both in surface modification of titanium and photoelectrical material but also provided a fundamental insight into the HAC mechanism in TNT stripping. These low cost approaches may be contributive to large-scale production in the future.

- Albu, S. P., Ghicov, A., Macak, J. M., Hahn, R. & Schmuki, P. Self-organized, Free-Standing TiO₂ Nanotube Membrane for Flow-through Photocatalytic Applications. *Nano Lett.* **7**, 1286–1289 (2007).
- Seayad, A. M. & Antonelli, D. M. Recent Advances in Hydrogen Storage in Metal-Containing Inorganic Nanostructures and Related Materials. *Adv. Mater.* **16**, 765–777 (2004).
- Yuan, R., Zhou, B., Hua, D. & Shi, C. Enhanced Photocatalytic Degradation of Humic Acids Using Al and Fe Co-doped TiO₂ Nanotubes under UV/Ozonation for Drinking Water Purification. *J. Hazard. Mater.* **262**, 527–538 (2013).
- Oh, S. *et al.* Significantly Accelerated Osteoblast Cell Growth on Aligned TiO₂ Nanotubes. *J. Biomed. Mater. Res. A* **78A**, 97–103 (2006).
- Balaur, E., Macak, J. M., Taveira, L. & Schmuki, P. Tailoring the Wettability of TiO₂ Nanotube Layers. *Electrochim. Commun.* **7**, 1066–1070 (2005).
- Guan, D., Hymel, P. & Wang, Y. Growth Mechanism and Morphology Control of Double-Layer and Bamboo-Type TiO₂ Nanotube Arrays by Anodic Oxidation. *Electrochim. Acta* **83**, 420–429 (2012).
- Mor, G. K., Shankar, K., Paulose, M., Varghese, O. K. & Grimes, C. A. Use of Highly-Ordered TiO₂ Nanotube Arrays in Dye-Sensitized Solar Cells. *Nano Lett.* **6**, 215–218 (2006).
- Popat, K. C., Eltgroth, M., LaTempa, T. J., Grimes, C. A. & Desai, T. A. Decreased Staphylococcus Epidermis Adhesion and Increased Osteoblast Functionality on Antibiotic-Loaded Titania Nanotubes. *Biomaterials* **28**, 4880–4888 (2007).
- Su, Z. & Zhou, W. Formation, Microstructures and Crystallization of Anodic Titanium Oxide Tubular Arrays. *J. Mater. Chem.* **19**, 2301–2309 (2009).

- Roy, P., Berger, S. & Schmuki, P. TiO₂ Nanotubes: Synthesis and Applications. *Angew. Chem. Int. Edit.* **50**, 2904–2939 (2011).
- Schmidt-Stein, F., Thiemann, S., Berger, S., Hahn, R. & Schmuki, P. Mechanical Properties of Anatase and Semi-Metallic TiO₂ Nanotubes. *Acta Mater.* **58**, 6317–6323 (2010).
- Wang, J. & Lin, Z. Freestanding TiO₂ Nanotube Arrays with Ultrahigh Aspect Ratio via Electrochemical Anodization. *Chem. Mater.* **20**, 1257–1261 (2008).
- Macak, J. M., Tsuchiya, H. & Schmuki, P. High-Aspect-Ratio TiO₂ Nanotubes by Anodization of Titanium. *Angew. Chem. Int. Edit.* **44**, 2100–2102 (2005).
- Kang, S. H., Kim, J. Y., Kim, H. S. & Sung, Y. E. Formation and Mechanistic Study of Self-Ordered TiO₂ Nanotubes on Ti Substrate. *J. Ind. Eng. Chem.* **14**, 52–59 (2008).
- Chen, Q. *et al.* Controlled Anodic Growth of TiO₂ Nanobelts and Assessment of Photoelectrochemical and Photocatalytic Properties. *Electrochim. Acta* **99**, 152–160 (2013).
- Shankar, K. *et al.* Highly-Ordered TiO₂ Nanotube Arrays up to 220 μm in Length: Use in Water Photoelectrolysis and Dye-Sensitized Solar Cells. *Nanotechnology* **18**, 065707 (2007).
- Yang, B. *et al.* Annealing Study of Titanium Oxide Nanotube Arrays. *Mater. Chem. Phys.* **130**, 1227–1231 (2011).
- Berger, S. *et al.* Influence of Water Content on the Growth of Anodic TiO₂ Nanotubes in Fluoride-Containing Ethylene Glycol Electrolytes. *J. Electrochem. Soc.* **157**, C18–C23 (2010).
- Lin, J. Y. *et al.* Effects of Rapid Thermal Annealing on the Structural Properties of TiO₂ Nanotubes. *Appl. Sur. Sci.* **258**, 530–534 (2011).
- Nishanthi, S. T., Iyyapushpam, S., Sundarakannan, B., Subramanian, E. & Pathinettam, D. Inter-Relationship Between Extent of Anatase Crystalline Phase and Photocatalytic Activity of TiO₂ Nanotubes Prepared by Anodization and Annealing Method. *Sep. Purif. Technol.* **131**, 102–107 (2014).
- Baradaran, S. *et al.* Fabrication and Deformation Behaviour of Multilayer Al₂O₃/Ti/TiO₂ Nanotube Arrays. *J. Mech. Behav. Biomed. Mater.* **20**, 272–282 (2013).
- Zalnezhad, E., Baradaran, S., Bushroa, A. R. & Sarhan, A. A. D. Mechanical Property Enhancement of Ti-6Al-4V by Multilayer Thin Solid Film Ti/TiO₂ Nanotubular Array Coating for Biomedical Application. *Metall. Mater. Trans. A* **45**, 785–797 (2014).
- Su, Z. & Zhou, W. Formation Mechanism of Porous Anodic Aluminium and Titanium Oxides. *Adv. Mater.* **20**, 3663–3667 (2008).
- Prakasam, H. E., Shankar, K., Paulose, M., Varghese, O. K. & Grimes, C. A. A New Benchmark for TiO₂ Nanotube Array Growth by Anodization. *J. Phys. Chem. C* **111**, 7235–7241 (2007).
- Taveira, L., Macak, J., Tsuchiya, H., Dick, L. & Schmuki, P. Initiation and Growth of Self-Organized TiO₂ Nanotubes Anodically Formed in NH₄F/NH₄SO₄ Electrolytes. *J. Electrochem. Soc.* **152**, 405–410 (2005).
- Paulin, I., Donik, C., Mandrino, D., Vončina, M. & Jenko, M. Surface Characterization of Titanium Hydride Powder. *Vacuum* **86**, 608–613 (2012).
- Simonsen, M. E., Jensen, H., Li, Z. & Sogaard, E. G. Surface Properties and Photocatalytic Activity of Nanocrystalline Titania Films. *J. Photochem. Photobiol., A* **200**, 192–200 (2008).
- Honjo, Y., Furuya, M., Takamasa, T. & Okamoto, K. Mechanism of Hydrophilicity by Radiation-Induced Surface Activation. *J. Power Energy Syst.* **3**, 216–227 (2009).
- Xu, C. *et al.* Molecular Hydrogen Formation from Photocatalysis of Methanol on TiO₂ 110. *J. Am. Chem. Soc.* **135**, 10206–10209 (2013).
- Lisowski, W., Van den Berg, A., Leonard, D. & Mathieu, H. Characterization of Titanium Hydride Films Covered by Nanoscale Evaporated Au layers: ToF-SIMS, XPS and AES depth profile analysis. *Sur. Interface Anal.* **29**, 292–297 (2000).
- Cao, Y., Yang, W., Chen, Y., Du, H. & Yue, P. Effect of Chemisorbed Surface Species on the Photocatalytic Activity of TiO₂ Nanoparticulate Films. *Appl. Sur. Sci.* **236**, 223–230 (2004).
- Iijima, M. *et al.* Corrosion Behavior of Ion Implanted Nickel-Titanium Orthodontic Wire in Fluoride Mouth Rinse Solutions. *Dent. Mater. J.* **29**, 53–58 (2010).
- Hack, J. & Leverant, G. The Influence of Microstructure on the Susceptibility of Titanium Alloys to Internal Hydrogen Embrittlement. *Metall. Trans. A* **13**, 1729–1738 (1982).
- Peddada, S., Robertson, I. & Birnbaum, H. Hydride Precipitation in Vapor Deposited Ti Thin Films. *J. Mater. Res.* **8**, 291–296 (1993).
- Lynch, S. Hydrogen Embrittlement Phenomena and Mechanisms. **30**, 105–123 (2012).
- Xu, X. *et al.* Tube-in-Tube TiO₂ Nanotubes with Porous Walls: Fabrication, Formation Mechanism, and Photocatalytic Properties. *Small* **7**, 445–449 (2011).
- Munoz, A. G. Semiconducting Properties of Self-Organized TiO₂ Nanotubes. *Electrochim. Acta* **52**, 4167–4176 (2006).
- Neamen, D. A. Metal-Semiconductor and Semiconductor Heterojunctions. *Semiconductor Physics and Devices: Basic Principles*. Butcher, K. (ed.) 326–366. (McGraw-Hill: New York, 2003).
- Lu, H. F. *et al.* Amorphous TiO₂ Nanotube Arrays for Low-Temperature Oxygen Sensors. *Nanotechnology* **19**, 405504 (2008).
- Fukai, Y. & Okuma, N. Evidence of Copious Vacancy Formation in Ni and Pd under a High Hydrogen Pressure. *Jpn. J. Appl. Phys.* **32**, 1256–1259 (1993).
- Li, F., Zhang, L. & Metzger, R. M. On the Growth of Highly Ordered Pores in Anodized Aluminum Oxide. *Chem. Mater.* **10**, 2470–2480 (1998).



42. Li, X., Liu, H., Yue, P. & Sun, Y. Photoelectrocatalytic Oxidation of Rose Bengal in Aqueous Solution Using a Ti/TiO₂ Mesh Electrode. *Environ. Sci. Technol.* **34**, 4401–4406 (2000).
43. Hondros, E. & Seah, M. Segregation to Interfaces. *Int. Met. Rev.* **22**, 262–301 (1977).
44. Ohtsuka, T., Guo, J. & Sato, N. Raman Spectra of the Anodic Oxide Film on Titanium in Acidic Sulfate and Neutral Phosphate Solutions. *J. Electrochem. Soc.* **133**, 2473–2476 (1986).
45. Brunner, E. Solubility of Hydrogen in 10 Organic Solvents at 298.15, 323.15, and 373.15 K. *J. Chem. Eng. Data* **30**, 269–273 (1985).

Acknowledgments

The authors acknowledge support for this research from the National High Technology Research and Development Program of China (2013AA032203, 2013AA031901), Outstanding Young Scholar Fund of Sichuan University (2014SCU04A20) and NSFC (31370971).

Author contributions

M.Z. and J.L. designed and performed all experiments and co-wrote the paper. J.W. and J.J. contributed to figure 4. Y.Z. contributed to the analysis of XPS. Y.L. and H.W. contributed to the correction and polish of the whole manuscript. All authors reviewed the manuscript.

Additional information

Supplementary information accompanies this paper at <http://www.nature.com/scientificreports>

Competing financial interests: The authors declare no competing financial interests.

How to cite this article: Zhao, M. *et al.* Gradient Control of the Adhesive Force between Ti/TiO₂ Nanotubular Arrays Fabricated by Anodization. *Sci. Rep.* **4**, 7178; DOI:10.1038/srep07178 (2014).



This work is licensed under a Creative Commons Attribution-NonCommercial-NoDerivs 4.0 International License. The images or other third party material in this article are included in the article's Creative Commons license, unless indicated otherwise in the credit line; if the material is not included under the Creative Commons license, users will need to obtain permission from the license holder in order to reproduce the material. To view a copy of this license, visit <http://creativecommons.org/licenses/by-nc-nd/4.0/>